

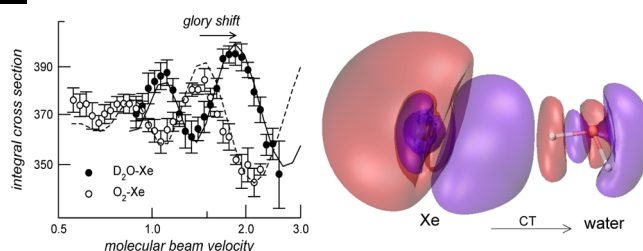
Revealing Charge-Transfer Effects in Gas-Phase Water Chemistry

DAVID CAPPELLETTI,^{*,†} ENRICO RONCA,[‡]
LEONARDO BelpASSI,[§] FRANCESCO TARANTELLI,^{*,‡,§} AND
FERNANDO PIRANI[‡]

[†]Dipartimento di Ingegneria Civile e Ambientale, Università di Perugia, Via G. Duranti 93, 06125 Perugia, Italy, [‡]Dipartimento di Chimica, Università di Perugia, Via Elce di Sotto 8, 06123 Perugia, Italy, and [§]CNR—Istituto di Scienze e Tecnologie Molecolari, Via Elce di Sotto 8, 06123 Perugia, Italy

RECEIVED ON FEBRUARY 29, 2012

CONSPECTUS



An understanding of the interactions involving water and other small hydrogenated molecules such as H₂S and NH₃ at the molecular level is an important and elusive scientific goal with potential implications for fields ranging from biochemistry to astrochemistry. One longstanding question about water's intermolecular interactions, and notably hydrogen bonding, is the extent and importance of charge transfer (CT), which can have important implications for the development of reliable model potentials for water chemistry, among other applications.

The weakly bound adducts, commonly regarded as pure van der Waals systems, formed by H₂O, H₂S, and NH₃ with noble gases or simple molecules such as H₂, provide an interesting case study for these interactions. Their binding energies are approximately 1 or 2 kJ/mol at most, and CT effects in these systems are thought to be negligible. Our laboratory has performed high-resolution molecular-beam scattering experiments that probe the (absolute scale) intermolecular potential of various types of these gas-phase binary complexes with extreme sensitivity. These experiments have yielded surprising and intriguing quantitative results. The key experimental measurable is the “glory” quantum interference shift that shows a systematic, anomalous energy stabilization for the water complexes and clearly points to a significant role for CT effects.

To investigate these findings, we have performed very accurate theoretical calculations and devised a simple approach to study the electron displacement that accompanies gas-phase binary intermolecular interactions in extreme detail. These calculations are based on a partial progressive integration of the electron density changes. The results unambiguously show that water's intermolecular interactions are not typical van der Waals complexes. Instead, these interactions possess a definite, strongly stereospecific CT component, even when very weak, where a water molecule may act as electron donor or acceptor depending on its orientation. CT is mediated by an asymmetric role played by the two hydrogen atoms, which causes strong orientation effects. The careful comparison of these calculations with the experimental results shows that the stabilization energy associated to CT is approximately 2–3 eV per electron transferred and may make up for a large portion of the total interaction energy. A simple electron delocalization model helps to validate and explain these findings.

1. Introduction

Water plays an essential role for life to thrive on our planet, as it constitutes the environment in which most biological processes take place. So, understanding at the molecular level the intermolecular interactions involving water is one

of the most important goals of science, but one which is still lamentably far from being accomplished.¹ It is certain that many biochemical processes depend on the special attributes of the water molecule and, in particular, on its ability to form directional, weak bonds which assist the

reorientation of three-dimensional structures.² Weak intermolecular bonds arise in general from the critical balance of some effective interaction components.³ Specifically, electrostatic (V_{electr}), induction (V_{ind}), and dispersion contributions (V_{disp}), which operate at long-range, combine with size-repulsion (V_{rep}) and charge-transfer effects (V_{CT}) which emerge at intermediate and short-range, being governed by the overlap of charge densities. For water, a very special, and crucially important, peculiarity is that of forming the so-called hydrogen bonding (HB).⁴ In extreme synthesis, the current view of HB⁵ is that many interaction components are present, but they may play a very different role in different systems. The manifestation and properties of hydrogen bonding have been intensely studied and are under ever closer scrutiny, but the list of open questions is still impressive. Some of these depend precisely on the lack of reliable, detailed information on the relative role of the various interaction components involved, particularly charge transfer (CT) and van der Waals ($V_{\text{vdW}} = V_{\text{rep}} + V_{\text{disp}}$).⁶ The role of charge transfer in HB is also of great relevance for dynamical processes such as the concerted proton–electron transfer.⁷ Very remarkably, similar questions apply to halogen bonding (XB), which recently started attracting a lot of attention.⁸ Indeed, the HB acceptor capabilities of the halogens and competition between HB and XB⁹ are issues of great interest and represent complementary aspects of a complex phenomenology.

An important characteristic of the components of non-covalent interactions is that they scale in a different way with the intermolecular distance r and vary with the geometry of the intermolecular complex they contribute to form. At large and intermediate distances, V_{electr} is often the dominant term, and the role of other contributions to the total interaction is difficult to ascertain accurately. The characterization of these terms is then best achieved by investigating systems where V_{electr} is absent or plays a minor role.

On these grounds, two decades ago¹⁰ the analysis of an ample range of systems involving closed-shell species (atoms, ions, and simple molecules) led us to establish correlation formulas which provide the basic features of the interaction (V_{vdW} and V_{ind}), in terms of polarizability and charge of the involved species. Subsequently, these results have been combined with extensive experimental and theoretical studies of systems formed by open-shell atoms with large electron affinity interacting with closed-shell partners. The various scattering and spectroscopic techniques employed for studying intermolecular interactions have been recently reviewed in ref 3. This allowed us to identify those systems where CT plays a relevant role.³ On the

basis of general criteria put forward in pioneering papers,^{11,12} we found¹³ that V_{CT} , the stabilization energy associated to CT effects, can be related to the ionization potential I of the electron donor, to the electron affinity A of the acceptor, and to the overlap integral S between the orbitals exchanging charge. The results of such investigations¹³ allowed us to map the transition from noncovalent intermolecular bonds, which arise from V_{vdW} plus possible V_{ind} and V_{electr} , to the simplest weak chemical bonds, where a perturbative CT stabilizes the aggregate, and finally to a one-electron chemical bond. Illustrative examples include heavier noble-gas halides and oxides, symmetric and asymmetric ionic noble gas dimers, and H_2^+ .

Recently, we have developed an integrated experimental and theoretical approach, which we shall review here, to reveal CT effects in weak intermolecular bonds and devoted particular effort to characterize especially water interactions. The systems studied include H_2O –noble gases (Ng),^{14,15} H_2O – H_2 ,¹⁶ NH_3 – H_2 , H_2O – O_2 and $-\text{N}_2$,¹⁷ H_2S –Ng,¹⁸ and NH_3 –Ng.^{19,20} The experimental data are obtained by molecular-beam scattering experiments, providing measurements of quantum interference structures in the collision cross section. A simultaneous analysis of the cross section magnitude and of the amplitude, frequency, and energy shift of its interference structure gives an accurate assessment of the absolute scale of the interaction and of the relative role of the various interaction components at play. An alternative approach exploits the measure of changes in nuclear quadrupole coupling constants upon complex formation.²¹ Gas-phase studies are ideal, because environmental effects are absent and a direct comparison with accurate computational simulations is possible.²¹ The latter are carried out using state-of-the-art ab initio methods, which provide assessment of both interaction energies and electron density rearrangements. In particular, an analysis of the charge displacement²² has proved to be very useful to cast light on the occurrence and extent of CT effects. As a final challenging task, we aimed at evaluating the energy associated with CT, thus taking the first firm steps toward the modeling of V_{CT} . This Account highlights some of the above experimental and theoretical achievements, including some new results and analysis aimed at further extending and generalizing our findings.

2. A Tale of Glory: Experimental Characterization of the Interaction

We first tackled the problem through molecular beam (MB) scattering experiments aimed at measuring, under high angular and velocity resolution conditions, the quantum

integral cross section Q as a function of the selected MB velocity, v . In the thermal velocity range, $Q(v)$ can be represented as the combination of an oscillatory pattern $\Delta Q(v)$, due to the “glory” quantum interference, superimposed to an average component, $\bar{Q}(v)$. These two observables provide complementary information on the intermolecular interaction: $\Delta Q(v)$ depends on the depth and location of the potential well while $\bar{Q}(v)$ is directly related to the strength of the long-range attraction. The experimental apparatus is composed by a MB source, a mechanical velocity selector, a scattering chamber containing the target, and a quadrupole mass spectrometer as detector.

Often we make our experiments using isotopically substituted species as projectile and target molecules. The elastic cross section data we measure are insensitive to the isotopic differences,¹⁶ but this has the advantage of improving both kinematic conditions and signal-to-noise ratio in the mass spectrometer. Overall, the better signal-to-noise ratio and the improved velocity resolution conditions appeared to be crucial to resolve the quantum interferences.

The cross sections are obtained by measuring the MB intensity with and without the gas target in the scattering chamber, applying the Lambert–Beer law and using an internal calibration for the target gas density. In our experiments, molecules are in thermal rotational and translational energy conditions; therefore, $Q(v)$ is mainly determined by elastic collisions and provides direct information on the spherically averaged interaction.¹⁵

On these grounds, we have undertaken the study of weakly bound, closed-shell, systems, involving water and/or other small hydrogenated molecules, aiming at measuring some effects due to the presence of HB. The approach is based on the simple idea to compare directly systems which share the same (ubiquitous) V_{vdW} terms but may differ for the presence of CT. The reference vdW systems, where we do not expect any HB effect, have been chosen making use of the predictions of the above-mentioned correlation formulas.¹⁰ As a relevant example, we illustrate the case of $\text{H}_2\text{O}-\text{X}$ systems (X is a noble gas atom or a simple molecule) as compared to $\text{Ar}-\text{X}$ and O_2-X , the vdW references. These complexes have a very similar spherically averaged interaction, arising from V_{vdW} plus V_{ind} . This can be understood on the basis of the average polarizability of water (1.47 \AA^3), which is only slightly smaller (by about 10%) than that of Ar (1.64 \AA^3) and of O_2 (1.60 \AA^3) and considering that the average induction in water–X adds an extra energy contribution, of about 10% of V_{disp} .¹⁶ Therefore, any measurable deviation of $\text{H}_2\text{O}-\text{X}$ from the expected behavior due to

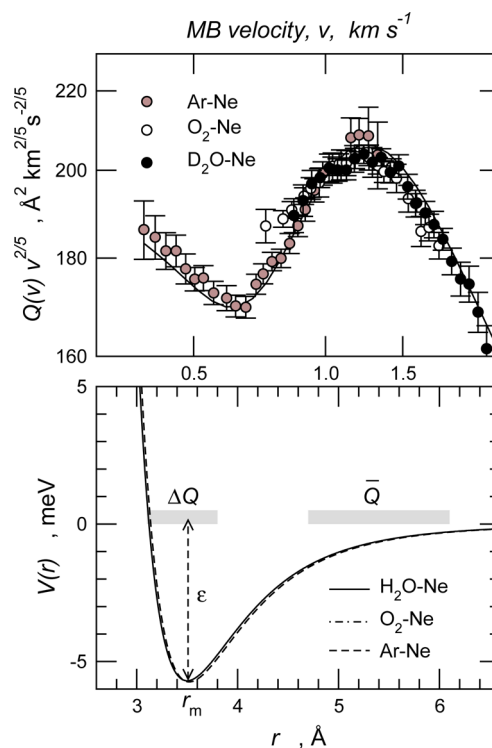


FIGURE 1. Upper panel: experimental cross sections Q for Ne–Ar, Ne– O_2 , and Ne– D_2O , as a function of MB velocity v . $Q(v)v^{2/5}$ is plotted to emphasize the quantum interference oscillations. The solid line represents the $\text{D}_2\text{O}-\text{Ne}$ cross sections calculated in the center-of-mass frame using the JWKB method and convoluted in the laboratory system for the direct comparison with experimental data.²³ Lower panel: best-fit experimental ILJ potentials. The potential parameters ϵ (well depth) and r_m (well location) are also indicated. The shaded areas evidence the distance ranges mainly probed by the experimental observables.²³

V_{vdW} plus V_{ind} can be attributed to the presence of additional interaction components. The same analysis suggests to use systems involving Kr as proper references for corresponding ammonia systems¹⁹ and those involving Xe for hydrogen sulphide systems.¹⁸

Figure 1 reports, in the upper panel, $Q(v)$ data measured under the same conditions for Ne– D_2O , Ne– O_2 , and Ne–Ar. The results are almost coincident, suggesting a very similar interaction potential for the three systems. This can be seen in the lower panel of the figure, where the best-fit potentials resulting from the analysis of the cross sections are displayed. The potentials extracted from the experiment are cast in analytic form using the improved Lennard-Jones (ILJ) model, whose formulation removes most of the limitations of the traditional Lennard-Jones function.²³ A discussion of the performance of the ILJ function and a critical comparison with other potential models is presented in ref 23. The comparison clearly indicates that, at all distances, the isotropic component of the intermolecular potential in

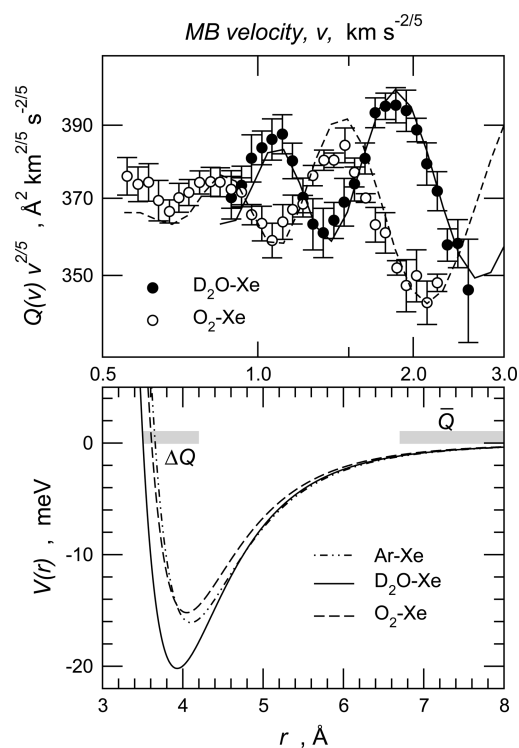


FIGURE 2. Upper panel: experimental and calculated cross sections Q for Xe–O₂ and Xe–D₂O. Lower panel: best-fit experimental ILJ potentials together with a Ar–Xe potential from the literature.²³ See also Figure 1.

neon–oxygen and neon–water basically depends, as in neon–argon, only on the combination of V_{vdW} and V_{ind} . The role of V_{CT} appears to be negligible.

The situation just illustrated for the Ne–water complex changes quite dramatically when we consider the corresponding Xe system. In Figure 2 we compare the cross section data for Xe–D₂O and Xe–O₂.

The magnitude of the cross section, \bar{Q} , is again very similar in the two complexes, an indication of the almost identical long-range attractive component. Eye-catching, however, is the large shift between the two glory interference patterns, which indicates the presence, in Xe–H₂O, of an additional binding force which emerges at intermediate distances, when the Xe and water electron clouds begin to overlap.¹⁴ This is clearly seen in the ILJ potential functions for the two systems extracted from the experimental data and plotted in the lower panel of Figure 2. For comparison, we show here also the potential for Xe–Ar.²³ This and the Xe–O₂ experimental potential are very similar, as expected, while the Xe–water complex exhibits a much more pronounced potential well depth. We attribute this extrastabilization to charge transfer, V_{CT} .

We have accumulated a growing collection of experimental observations, providing the dependence of CT on

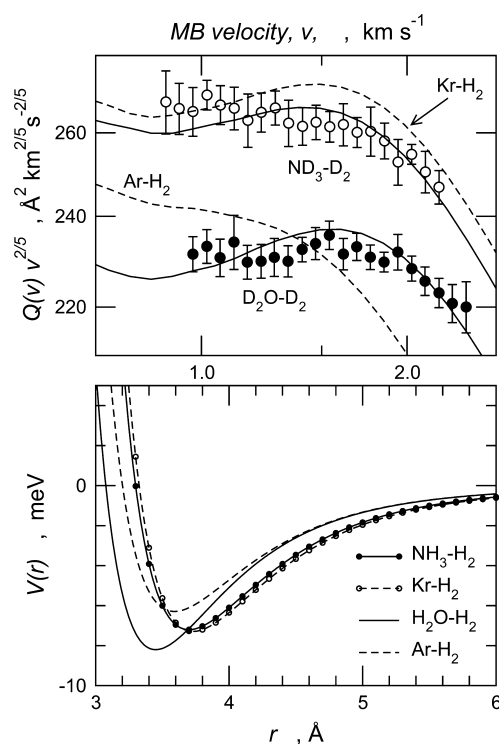


FIGURE 3. Upper panel: experimental cross sections and best fit ILJ potentials (solid lines) for ND₃–D₂ and D₂O–D₂. Dashed lines are cross sections for Kr–H₂ and Ar–H₂ calculated from accurate computed potential energy surfaces.^{10,16} Lower panel: best fit experimental spherical (ILJ) potentials for ND₃–D₂ and D₂O–D₂, together with literature potentials for Kr–H₂ and Ar–H₂.^{10,16}

the Ng and also comparing water with other hydrides, which confirm the above conclusions and the peculiarity of the interactions involving water.^{14,15,17–20} As an example, we briefly illustrate here the data obtained for the NH₃–H₂ and H₂O–H₂ systems, shown in Figure 3. For comparison, we also show theoretical data for Kr–H₂ and Ar–H₂. Here we notice that the cross section magnitude is similar for Kr–H₂ and ND₃–D₂, and it is larger for these systems than for Ar–H₂ and D₂O–D₂; the latter two are also comparable with each other. As explained earlier, this is a measure of the stronger long-range attraction in the former two systems and essentially reflects the pattern of polarizabilities.¹⁰ Polarizability is similar for ammonia (2.16 \AA^3) and Kr (2.49 \AA^3) and also similar, but roughly 50% smaller, for water (1.47 \AA^3) and Ar (1.64 \AA^3).¹⁰ It is however evident that the Kr and ammonia complexes exhibit also a nearly identical glory oscillation in the cross section, while the water complex is again anomalous, since the glory hump in its cross section is noticeably shifted to higher velocity compared to Ar. Again, this is a consequence of the emergence of an additional attractive force at intermediate range in the water complex which, in spite of the slightly weaker long-range attraction,

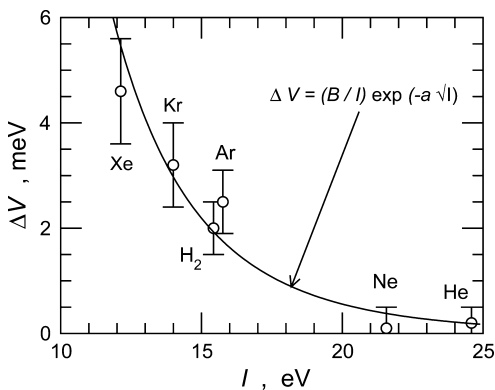


FIGURE 4. Experimentally determined bond stabilization ΔV due to CT (see text) for some water complexes, reported as a function of the ionization potential I of the donor partner. The data exhibit an exponential dependence on \sqrt{I} .

causes a significant deepening of the potential well (see the lower panel of Figure 3). This comparison thus suggests that V_{CT} plays an important role in water–hydrogen¹⁶ but is nearly undetectable in ammonia–hydrogen.

We may attempt a semiempirical rationalization of the stronger binding observed in the water binary complexes. Let us define a stabilization energy ΔV as the difference in the experimentally determined well depth ε between a water complex with partner X and the corresponding averaged reference X–Ar and X–O₂ system.

Figure 4 reports ΔV for six cases, the noble-gas and the hydrogen complexes, as a function of the ionization potential, I , of X. In this context, our results may be considered to fall in the asymptotic region of the phenomenology discussed recently by Legon²¹ in an analysis of systems involving typical hydrogen and halogen bonds. The data points in the plot appear to be reasonably well fitted with an exponential function of \sqrt{I} . This is in line with an analysis of open-shell atomic systems^{3,13} and with the radial exponential dependence of the overlap integral S promoting CT.^{11,12} The pre-exponential factor also depends on I^{-1} , which accounts for the energy gap between the states coupled by CT.¹³

3. How To Define and Measure CT? A Model for CT Energy Stabilization

To put on firm theoretical grounds the experimental observations and the analysis reviewed above requires a way to assess and compute reliably the occurrence of quite small CT phenomena. A priori, this poses a significant dilemma, over and above the problem of adopting a theoretical framework accurate enough to provide an adequate description of weak intermolecular interactions. Indeed, interpreting and

predicting the electronic structure, properties, and even reactivity of chemical systems in terms of the partial transfer of electronic charge from one species to another is one of the oldest, simplest, and unquestionably most useful tools of chemists—experimentalists and theoreticians alike. And yet, CT extent and effects remain often elusive and hotly debated, especially in weak interactions, because a rigorous, unique, first-principles definition of CT does not (and cannot) exist. There are, no doubt, several well-established and widely used charge decomposition models,^{24–26} devised to assign partial charges or CT energies, but it is not uncommon that, especially in cases where CT is very small, they give different and even conflicting results, leaving room to doubts and open questions. We have therefore proposed a different approach to tackle the problem, which offers a somewhat broader perspective in which to assess the occurrence of CT, free of any charge decomposition scheme. This is based on the key idea of a *charge-displacement* (CD) function,²² defined as

$$\Delta q(z) = \int_{-\infty}^{\infty} dx \int_{-\infty}^{\infty} dy \int_{-\infty}^z \Delta \rho(x, y, z') dz' \quad (1)$$

Here z is any chosen axis of interest, typically one joining the interacting species, and $\Delta \rho$ is the change in electron density taking place upon formation of the intermolecular complex, i.e. the density difference between the complex and the isolated noninteracting partners placed at the same positions they occupy in the complex.²⁷ Clearly, $\Delta q(z)$ measures, at each point z along the axis, the electron charge that, upon formation of the adduct, has crossed from right to left the plane through z perpendicular to the axis. This provides a concise, obviously limited, but insightful snapshot of the whole electron cloud rearrangement arising from all the interaction components.

Especially for weakly bound systems, the evaluation of $\Delta q(z)$ along an axis joining the interacting species is immediately helpful for a qualitative assessment of the occurrence and extent of CT, because the curve obviously suggests CT when it is appreciably different from zero and does not change sign in the region between the fragments, whereas CT may be uncertain (in both magnitude and direction) if the curve crosses zero. When CT takes place, it may be useful for many comparative purposes to come up with some definite numerical estimate of it, which can simply be done by taking the value of the CD curve at some specific point between the fragments, i.e. define a plane separating them. This is, of course,

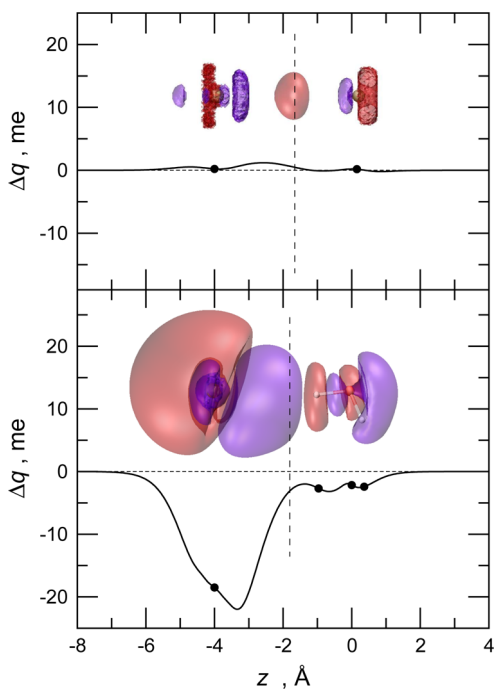


FIGURE 5. Charge-displacement curves describing the formation of Xe–Ar (upper panel) and Xe–H₂O (lower panel). 3D contour plots of the electron density change accompanying bond formation are also shown. The isodensity surfaces are for $\Delta\rho = \pm 0.03$ me/bohr³ (negative value in red, positive in blue). The dots on the Δq curves correspond to the positions of nuclei on the z axis, which is here the axis joining Xe with the center of mass (c.m.) of the interacting partners. The axis origin is at the c.m. of water and Ar, respectively. The vertical dashed lines mark the isodensity boundaries between the fragments.

a matter of convention, but again here, the CD function itself, in particular its shape and slope around the chosen separation point, is quite helpful to assess the meaningfulness of one's choice. If the curve is sufficiently flat between the fragments, the exact position of the boundary between them is not critical, while more caution and analysis may be required otherwise. As a reasonable model, in our previous work, we have usually chosen to separate the fragments and extract the CT value at their so-called isodensity boundary, i.e., the point along z where the electron densities of the noninteracting fragments become equal. We have often noticed that this point turns out to be close to the minimum of the total molecular density between the fragments, and also close to the bond critical point²⁸ when there is one.

As an example, Figure 5 compares the CD curves obtained for Xe–Ar, a prototypical van der Waals (VdW) complex, and Xe–H₂O at its equilibrium geometry, for which, as discussed above, the experiments reveal a pronounced additional intermolecular bond stabilization. Details of the calculations are given in the Supporting

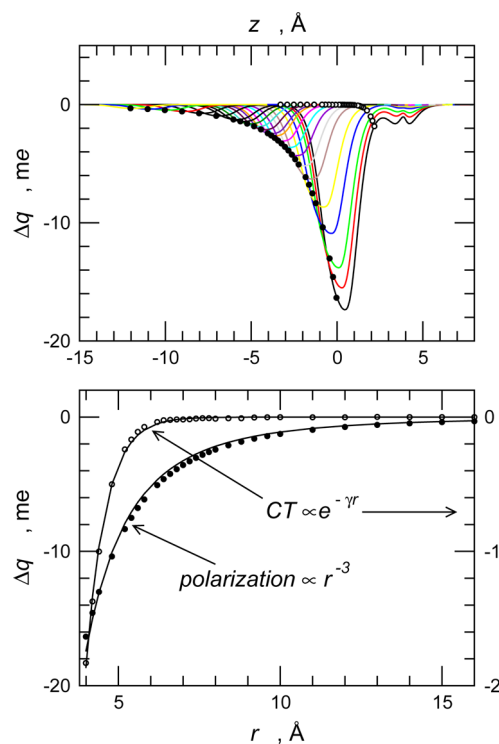


FIGURE 6. Upper panel: CD curves for different distances (r) between Xe and water's c.m., with Xe lying on the water's C_{2v} axis on the hydrogen side. r ranges between 4.0 Å (black line), which corresponds to the energy minimum, and 16.0 Å. Filled circles correspond to Xe position and empty circles to isodensity boundary. Lower panel: Best fit of Δq values at Xe position and at isodensity boundary as a function of r .

Information (SI). One notices immediately the large qualitative difference between the two Δq curves. The former is very close to zero everywhere and changes sign between the fragments (in fact, very close to the isodensity boundary). The latter, besides being dominated by the strong Xe polarization due to water's dipole, shows unambiguously the qualitative signature of CT, being distinctly different from zero and of the same sign everywhere, in fact not only between the fragments but all the way across the entire molecular aggregate. A detailed analysis of the CD functions for the whole series of water–noble-gas complexes has been reported in ref 14. We recall here, in particular, the important finding of the asymmetric, concerted role of both hydrogen atoms (one electron acceptor and the other electron donor) in mediating CT (in this case from the noble gas to water). In addition, Δq curves computed at different orientations show that the amount and even direction of CT may be strongly anisotropic,^{14,16} with the water molecule acting mostly as electron acceptor but also as a donor in some configurations of specific H₂O–X complexes (X = Kr, Xe, and H₂). Figure 5 also shows that the choice of the isodensity boundary to fix a CT value is not problematic in Xe–H₂O. Moving the boundary toward water would not alter the

CT value significantly, while moving it in the opposite direction would increase CT unrealistically, as it would penetrate the evident large electron cloud polarization around Xe.

As we recalled earlier, the interaction components scale differently with distance. In particular, because it depends on the overlap between the electron clouds of the fragments, CT should fall off exponentially with distance. To explore this point, we examine the dependence of the $\Delta q(z)$ function on the Xe–H₂O distance (for a fixed orientation), focusing, for comparison, on two specific points: the isodensity boundary, where, as put forward above, Δq should essentially represent CT, and the z position of the Xe atom, where charge displacement should be dominated by polarization effects.

The two CD values show indeed a qualitatively different dependence on r , as evidenced in the lower panel of Figure 6. At the Xe atom, Δq decreases with an r^{-3} dependence (the best fit would yield $r^{-2.7}$). This confirms that it is indeed a measure of Xe polarization caused by the presence of water, as it scales as the classical induced dipole on Xe ($\mu_{\text{ind,Xe}} \sim \alpha_{\text{Xe}} \mu_{\text{w}} r^{-3}$, where α_{Xe} is Xe polarizability and μ_{w} the magnitude of water dipole). By contrast, at the isodensity point, Δq falls off exponentially, as one expects for CT. It is interesting that the model mentioned earlier,¹³ in which the energy stabilization due to CT also decays as $e^{-\gamma r}$, with γ proportional to the square root of the ionization potential of the donor, would yield, in the Xe–H₂O case, $\gamma = 1.78 \text{ \AA}^{-1}$, matching fairly well the γ value of 1.6 \AA^{-1} that we obtain from the best fit of the computed CT decay. This is consistent with the simple expectation that CT and the energy associated with it are proportional.^{25,26}

Having established a well-defined method to assess CT computationally, how can we make contact with the experimental observation of an energy stabilization attributed to it? We have successfully tackled this question in a work on the water–H₂ complex¹⁶ and we use the same approach here. Note that, since Xe has no permanent multipole, the picture is not complicated by the presence of V_{electr} . The analysis of the Xe–H₂O cross section measurements provides the accurate radial (orientationally averaged) dependence of the interaction potential. To evaluate from the calculations the part of this potential arising from CT, we need to estimate the radial dependence of the computed CT magnitude (i.e., regardless of direction), averaged over the orientations of the interacting partners. As detailed in ref 16 and in the SI, it is not difficult to obtain such an estimate, expressed as $\overline{CT}(r)$. Assuming now that the corresponding energy contribution

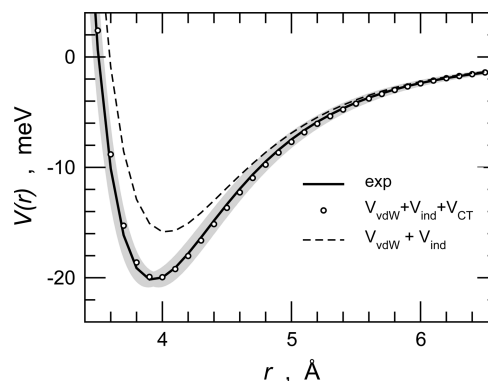


FIGURE 7. Experimental isotropic interaction potential for Xe–H₂O (solid line). V_{vdW} is calculated assuming a ILJ functional form with parameters $r_m = 4.07 \text{ \AA}$ and $\varepsilon = 13.9 \text{ meV}$.¹⁰ V_{ind} is the rotationally averaged induction contribution estimated as $\mu_{\text{w}}^2 \alpha_{\text{Xe}} r^{-6}$. V_{CT} is given by eq 2 with $k = 2.6 \text{ eV/e}$. The gray region shows the experimental uncertainty.

is proportional to it,^{25,26}

$$V_{\text{CT}}(r) = k \overline{CT}(r) \quad (2)$$

we can check if this function, with the sole parameter k , the energy per transferred unit charge, summed to the model $V_{\text{vdW}}(r)$ and $V_{\text{ind}}(r)$ components, can provide a reasonable fit of the experimentally determined potential.

This is shown in Figure 7, and it clearly appears to be remarkably accurate over the whole r range considered. It provides values for the well position and depth of $r_m = 3.95 \text{ \AA}$ and $\varepsilon = 20.06 \text{ meV}$, respectively, essentially coincident with the experimentally determined values ($r_m = 3.93 \text{ \AA}$, $\varepsilon = 20.20 \text{ meV}$).¹⁵ Clearly, these findings strongly support the conclusion that the difference between the experimentally determined isotropic interaction potential and that expected on the basis of the sole vdW plus induction forces is indeed due to CT.

The best-fit parameter value for V_{CT} in Xe–H₂O is $k = 2.6 \text{ eV/e}$ and, remarkably, turns out to be essentially identical to that extracted with the same procedure for other water–noble-gas systems and in the H₂–H₂O case ($k = 2.5 \text{ eV}$).¹⁶ With this parameter we can estimate that, at the most stable configuration of the Xe–H₂O system, V_{CT} is about 10 meV, or about 40% of the total interaction energy. It may be of interest to observe that the CT energy stabilization we have thus determined is roughly of the same magnitude as that one can estimate using a recently proposed procedure,²⁹ from symmetry adapted perturbation theory (SAPT).³⁰ In this theory, the CT energy is not explicit but hidden behind various well-defined energy terms. However, by applying the mentioned procedure,²⁹ we estimate a CT contribution of 6–7 meV (see the SI for details).

4. Physical Origin of the CT Energy Stabilization

On the basis of the present and other calculations,¹⁶ the stabilization energy arising from CT appears to be characterized by the roughly constant rate of 2–3 eV per electron transferred across a wide range of water complexes. Where does this nearly constant energy value come from? Can we devise an independent model to help us rationalize the origin and magnitude of this stabilization, and thereby assess the validity of our approach and conclusions?

It is immediately clear that a crude electrostatic picture, in which one thinks of the CT energy as the Coulomb interaction of the positive and negative excess charges created by the CT process, would yield energy values that, besides depending on the square of the charge rather than the first power, are wrong by orders of magnitude. For example, the classical Coulomb energy associated to two opposite point charges of 3.9 me (the amount of CT from Xe to water that we computed) placed 4.0 Å apart (the computed Xe–H₂O equilibrium distance) is over 2 orders of magnitude smaller than the 10 meV we have found for this complex. In a more realistic model, in which the two point charges are replaced by charge distributions, the energy would be even smaller.

But if the interaction energy of the excess charges contributes negligibly, what is the true source of stabilization associated with CT? The extended charge displacement seen in Figure 5 suggests that CT results in some amount of electron sharing between the interacting fragments. While in an isolated Xe atom the electrons are confined to this fragment, in the complex with water a fraction of electrons becomes delocalized over the whole system. In other words, the formation of the complex increases the space available to the electrons, which results in a kinetic energy decrease. Electron sharing constitutes the fundamental mechanism of covalent bond formation, and the associated kinetic energy decrease plays a crucial role in stabilizing the system.^{31,32} It is well-recognized, for example, that this is the mechanism entirely responsible for the covalent bond formation in H₂⁺.³¹

The decrease in the quantum-mechanical kinetic energy is exemplified by the case of a free particle in a box when the size of the box is increased. Let us examine this simplest of models, adapting it to the size of the Xe–H₂O system. If we describe the space available to the electrons of the Xe atom as a cubic box of side L_{Xe} , the change in the ground state energy of a free electron within the box when its length is

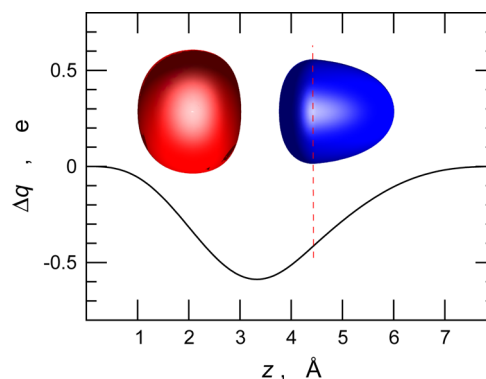


FIGURE 8. CD curve describing the delocalization of a free ground state electron, initially confined to a volume approximately equal to that of a Xe atom (on the left), when the box is increased to the volume of the Xe–H₂O complex (see text). Two 3D isosurfaces of the density change, of value ± 3 me/bohr³ (red is negative), are also shown. The vertical dashed line identifies the z position of the right face of the “Xe box”.

increased in one direction by the quantity L_w (the side of a “water box”) is given by (in atomic units):

$$\Delta E = \frac{\pi^2}{2} \left[\frac{1}{(L_{\text{Xe}} + L_w)^2} - \frac{1}{L_{\text{Xe}}^2} \right] \quad (3)$$

We may roughly estimate L_{Xe} by doubling the Xe radius obtained by subtracting half of the Ar–Ar distance in Ar₂ (3.8 Å) from the Xe–Ar distance (4.1 Å), yielding $L_{\text{Xe}} = 4.4$ Å. A similar calculation using the Xe–H₂O isotropic well position gives $L_w = 3.4$ Å. When we use these values in eq 3, we obtain a kinetic energy decrease of 1.3 eV.

Figure 8 shows the CD curve associated with the free electron delocalization just described along with the corresponding 3D contour plot of the density change, where the free-electron wave function for a box of side L is of the form

$$\psi(x, y, z) = \sqrt{\frac{8}{L^3}} \sin \frac{\pi x}{L} \sin \frac{\pi y}{L} \sin \frac{\pi z}{L} \quad (4)$$

As usual, we take the amount of CT from the “Xe box” to the “water box” as the CD value at the boundary between the two boxes, which is 0.37 electrons. This means that the energy stabilization associated with this delocalization is 3.5 eV per electron transferred, a value surprisingly consistent with our findings for the water intermolecular complexes and displaying the correct dependence on CT.

5. Conclusions

We have reviewed in this paper how state-of-the-art scattering experiments combined with a simple, well-designed theoretical approach can tame and bring into a useful perspective—amenable to modeling—the elusive and

controversial subject of charge-transfer effects in weak intermolecular interactions, a particularly promising endeavor to better understand the origin of fundamental and much debated interactions, such as the hydrogen bond and the halogen bond.⁹ We have shown that it is possible to measure experimentally, and reliably estimate by theory, the energy stabilization associated to CT, which turns out to be of the order of 2–3 eV per electron transferred in several binary water adducts. This is a far from negligible figure, that may make up for a large fraction of the total interaction energy when electrostatic forces are weak, and may therefore drive the geometry of the interaction. Using a simple model, we surmise that, to a large extent, the most likely explanation for this energy component must be essentially the same as that which accounts, in large part, for covalent bond formation, namely the electron kinetic energy decrease associated to electron delocalization (sharing).

This work was supported by the MIUR (PRIN project no. 2008KJX4SN_003).

Supporting Information. Details of the calculations, comparison with other CT evaluation methods, evaluation of the SAPT CT energy, and evaluation of the average radial dependence of CT in Xe–H₂O. This material is available free of charge via the Internet at <http://pubs.acs.org>.

BIOGRAPHICAL INFORMATION

David Cappelletti was born in Locarno, Switzerland, in 1965. Currently he is associate professor at the University of Perugia. His research interests include intermolecular forces, surface physics, snow chemistry, and atmospheric aerosols.

Enrico Ronca was born in Acquapendente, Italy, in 1987. He is currently a Ph.D. student at the University of Perugia, where he works mainly at the analysis of the charge displacement accompanying excitation in photovoltaics materials.

Leonardo Belpassi was born in Foligno, Italy, in 1977. Currently he is researcher at CNR-ISTM, Perugia. His research interests include electronic structure calculations, relativistic effects, and chemical bonding.

Francesco Tarantelli was born in Porto San Giorgio, Italy, in 1956 and has been full professor at the University of Perugia, since 2000. His research activity, in theoretical and computational chemistry, extends over a wide variety of subjects, including electron spectroscopy, intermolecular interactions, relativistic quantum chemistry, algorithms, and high-performance computing.

Fernando Pirani was born in Fabriano (Italy) in 1949. Currently he is full professor at the University of Perugia. His research interests encompass the determination of intermolecular potentials via integral cross section measurements and the development of correlation formulas, alignment effects, gas-surface interactions,

solvation phenomena, and photoionization processes studied with synchrotron light.

FOOTNOTES

*To whom correspondence should be addressed. E-mail: david.cappelletti@unipg.it; franc@thch.unipg.it.

The authors declare no competing financial interest.

REFERENCES

- Special Issue: Water in chemistry. *Acc. Chem. Res.* 2012, 45, 1–138.
- Ball, P. Water as an active constituent in cell biology. *Chem. Rev.* 2008, 108, 74–108.
- Pirani, F.; Maciel, G.; Cappelletti, D.; Aquilanti, V. Experimental benchmarks and phenomenology of interatomic forces: open-shell and electronic anisotropy effects. *Int. Rev. Phys. Chem.* 2006, 25, 165–199.
- Jeffrey, J. *An Introduction to Hydrogen Bonding*; Oxford University Press: Oxford, 1997.
- Arunan, E.; Desiraju, G.; Klein, R.; Sadlej, J.; Scheiner, S.; Alkorta, I.; Clary, D.; Crabtree, R.; Dannenberg, J.; Hobza, P.; Kjaergaard, H.; Legon, A.; Mennucci, B.; Nesbitt, D. Definition of the hydrogen bond (IUPAC Recommendations 2011). *Pure Appl. Chem.* 2011, 83, 1637–1641.
- We define the van der Waals interaction as due to the combination of long-range dispersion and induction attraction with short-range size repulsion. Other slightly different definitions have also been proposed.
- Proton Coupled Electron Transfer. Thematic Issue. *Chem. Rev.* 2010, 110, 6937–7100.
- Metrangolo, P., Resnati, G., Eds. *Halogen bondings: fundamentals and applications*; Springer: Berlin, 2008.
- Cappelletti, D.; Candori, P.; Pirani, F.; Belpassi, L.; Tarantelli, F. Nature and Stability of Weak Halogen Bonds in the Gas Phase: Molecular Beam Scattering Experiments and Ab Initio Charge Displacement Calculations. *Cryst. Growth Des.* 2011, 11, 4279–4283.
- Cambi, R.; Cappelletti, D.; Liuti, G.; Pirani, F. Generalized correlations in terms of polarizability for van der Waals interaction potential parameter calculations. *J. Chem. Phys.* 1991, 95, 1852.
- Magee, J. The Mechanism of Reactions Involving Excited Electronic States The Gaseous Reactions of the Alkali Metals and Halogens. *J. Chem. Phys.* 1940, 8, 687–698.
- Grice, R.; Herschbach, D. Long-range configuration interaction of ionic and covalent states. *Mol. Phys.* 1974, 27, 159–175.
- Pirani, F.; Giulivi, A.; Cappelletti, D.; Aquilanti, V. Coupling by charge transfer: role in bond stabilization for open-shell systems and ionic molecules and in harpooning and proton attachment processes. *Mol. Phys.* 2000, 98, 1749–1762.
- Belpassi, L.; Tarantelli, F.; Pirani, F.; Candori, P.; Cappelletti, D. Experimental and theoretical evidence of charge transfer in weakly bound complexes of water. *Phys. Chem. Chem. Phys.* 2009, 11, 9970–9975.
- Roncaratti, L.; Belpassi, D.; Cappelletti, D.; Pirani, F.; Tarantelli, F. Molecular-Beam Scattering Experiments and Theoretical Calculations Probing Charge Transfer in Weakly Bound Complexes of Water. *J. Phys. Chem. A* 2009, 113, 15223–15232.
- Belpassi, L.; Recca, M.; Tarantelli, F.; Roncaratti, L.; Pirani, F.; Cappelletti, D.; Faure, A.; Scribano, Y. Charge-Transfer Energy in the Water-Hydrogen Molecular Aggregate Revealed by Molecular-Beam Scattering Experiments, Charge Displacement Analysis, and ab Initio Calculations. *J. Am. Chem. Soc.* 2010, 132, 13046–13058.
- Cappelletti, D.; Candori, P.; Roncaratti, L.; Pirani, F. A molecular beam scattering study of the weakly bound complexes of water and hydrogen sulphide with the main components of air. *Mol. Phys.* 2010, 108, 2179–2185.
- Pirani, F.; Candori, P.; Pedrosa Mundim, M.; Belpassi, L.; Tarantelli, F.; Cappelletti, D. On the role of charge transfer in the stabilization of weakly bound complexes involving water and hydrogen sulphide molecules. *Chem. Phys.* 2012, 398, 176–185.
- Pirani, F.; Roncaratti, L.; Belpassi, L.; Tarantelli, F.; Cappelletti, D. Molecular-beam study of the ammonia-noble gas systems: Characterization of the isotropic interaction and insights into the nature of the intermolecular potential. *J. Chem. Phys.* 2011, 135, No. 194301.
- Bistoni, G.; Belpassi, L.; Tarantelli, F.; Pirani, F.; Cappelletti, D. Charge-displacement analysis of the interaction in the ammonia noble gas complexes. *J. Phys. Chem.* 2011, 115, 14657–14666.
- Legon, A. The halogen bond: an interim perspective. *Phys. Chem. Chem. Phys.* 2010, 12, 7736–7747.
- Belpassi, L.; Infante, I.; Tarantelli, F.; Visscher, L. The Chemical Bond between Au(I) and the Noble Gases. Comparative Study of NgAuF and NgAu⁺ (Ng = Ar, Kr, Xe) by Density Functional and Coupled Cluster Methods. *J. Am. Chem. Soc.* 2008, 130, 1048–1060.
- Pirani, F.; Brizi, S.; Roncaratti, L. F.; Casavecchia, P.; Cappelletti, D.; Vecchiocattivi, F. Beyond the Lennard-Jones model: a simple and accurate potential function probed by high

- resolution scattering data useful for molecular dynamics simulations. *Phys. Chem. Chem. Phys.* **2008**, *10*, 5489–5503.
- 24 Mulliken, R. S. Electronic Population Analysis on LCAO-MO Molecular Wave Functions. I. *J. Chem. Phys.* **1955**, *23*, 1833–1840.
- 25 Reed, A. E.; Curtiss, L. A.; Weinhold, F. Intermolecular interactions from a natural bond orbital, donor-acceptor viewpoint. *Chem. Rev.* **1988**, *88*, 899–926.
- 26 Khaliullin, R. Z.; Bell, A. T.; Head-Gordon, M. Analysis of charge transfer effects in molecular complexes based on absolutely localized molecular orbitals. *J. Chem. Phys.* **2008**, *128*, No. 184112.
- 27 This definition includes the change in density due to the antisymmetrization and renormalization of the total wave function made up from the nonorthogonal fragment wave functions.
- 28 Bader, R. F. W. A quantum theory of molecular structure and its applications. *Chem. Rev.* **1991**, *91*, 893–928.
- 29 Stone, A. J.; Misquitta, A. J. Charge-transfer in Symmetry-Adapted Perturbation Theory. *Chem. Phys. Lett.* **2009**, *473*, 201–205.
- 30 Jeziorski, B.; Moszyński, R.; Szalewicz, K. Perturbation Theory Approach to Intermolecular Potential Energy Surfaces of van der Waals Complexes. *Chem. Rev.* **1994**, *94*, 1887–1930.
- 31 Ruedenberg, K.; Schmidt, M. W. Physical Understanding through Variational Reasoning: Electron Sharing and Covalent Bonding. *J. Phys. Chem. A* **2009**, *113*, 1954–1968.
- 32 Kutzelnigg, W. The Physical Mechanism of the Chemical Bond. *Angew. Chem., Int. Ed. Engl.* **1973**, *12*, 546–562.